Journal of Soil Salinity and Water Quality 18(1), 70-78, 2026
DOI: https://doi.org/10.56093/jsswq.v18i1.175856

Remediation of Cationic Dye from Waste Water using Low Cost Biosorbent: Preparation, Characterization, Adsorption Study

Manju[1], Sachin Kumari[1*], Bhagya Shree[1], Sushila Singh[1] and Ankush Dhanda[2]

[1]*Department of Chemistry, Chaudhary Charan Singh Haryana Agricultural University, Hisar-125004, Haryana, India*
[2]*Department of Soil Science, Chaudhary Charan Singh Haryana Agricultural University, Hisar-125004, Haryana, India*
**Corresponding author E-mail: sachindalal@hau.ac.in*

Abstract

Human and aquatic health is frequently at risk due to dye pollution in aquatic environments. In order to remediate water contaminated with cationic dye namely brilliant green (BG) dye, a chemically modified almond shell adsorbent was developed in the present study. The physico-chemical characteristics of modified almond shell (MAS) were investigated using a variety of characterization techniques, including *p*Hpzc, FTIR, FE-SEM, and EDS. Studies have been conducted on the impacts of different adsorption parameters, including the *p*H, dye concentrations, adsorbent dose, contact time and temperature. The optimized conditions were *p*H-8, 0.8 g/L of adsorbent dose, 120 minutes of contact time and temperature 50° C. The BG uptake by modified almond shell was explained by the monolayer adsorption onto energetically equivalent sorption sites. The Langmuir model yielded a maximal adsorptive capacity of 121.73 mg BG per g MAS. The kinetic models also showed that the rate depends on the adsorbent's adsorptive capacity. The pseudo-second-order model fits BG adsorption well, with R2 > 0.99. Thermodynamic studies indicated that adsorption is feasible, spontaneous, and endothermic. This work suggests that MAS warrants further investigation as a potential adsorbent for removing BG dye.

Keywords: Almond shell, Adsorption, Cationic dye, Isotherm studies

Introduction

Water contamination is mostly caused by industrial dye effluents from plastics, textiles, leather, and cosmetics. In addition to having an adverse effect on aquatic ecosystems, dye-polluted water is a major cause of respiratory infections, skin irritation, mental illness, and numerous other public health issues (Jadhav *et al.*, 2010). The textile sector alone accounts for two-thirds of the world's dyestuff production (Sahu and Poler, 2024). Brilliant green is a common dye used in the pulp, paper, and dyeing industries to provide intense green hues. It is also used as an antibacterial and antiseptic (Nandi *et al.*, 2009). Brilliant Green is a cationic dye that is far more toxic than other anionic dyes due to the presence of azo and amine compounds, which can result in hazardous breakdown products and pose a health risk to humans when consumed or come into contact with them (Nhat Ngo *et al.*,2026). BG irritates the skin, respiratory system, and gastrointestinal tract, resulting in symptoms including diarrhea, nausea and stomach pain (Roy *et al.*, 2018). Conventionally employed techniques for eliminating inorganic and organic contaminants from water include chemical precipitation, ion exchange, membrane filtration, coagulation and adsorption (Zhao *et al.*, 2020). Adsorption techniques offer the benefits of adaptability in application and simplicity in design that prevents the formation of hazardous intermediates (Manzoor *et al.*, 2024). Numerous types of forestry and agricultural waste, including lignin, rice husk, pine core, chestnut shell etc., have reportedly been employed as environmentally beneficial adsorbents (Xu *et al.*, 2017). Of these, almond shell powder (ASP) has drawn the most attention lately because of its outstanding adsorption capability for the removal of colours and its widespread availability (Lima *et al.*, 2019). The production of almonds generates a lot of waste, which is typically burned or dumped in landfills because of almonds' widespread use as food. Because buried almond shells are so hard and take so long to break down, they create an environmental hazard (Miyah *et al.*, 2018).

Here, alkali-gluteraldehyde-treated almond shell, an appropriate adsorbent, was prepared for BG adsorption from aqueous solutions. The adsorption mechanism and kinetics of BG were also investigated in this work, and several physicochemical parameters that influence the adsorption rate and the amount adsorbed were identified. Adsorption was investigated in relation to solution *p*H, initial dye concentration, adsorbent dose, contact time, and temperature. This research was conducted in Department of Chemistry & Soil sciences, C.C.S.H.A.U. Hisar, Haryana.

Material and Methods

The BG dye removal tests and the almond shell modifications were carried out using analytical-grade chemicals from Hi-media Laboratory Pvt. Ltd. The biomass made from almond shells (AS) was purchased from the local market in Hisar, Haryana, India. To obtain the required particle size, the dry almond shells were crushed and sieved through a 40–60-mesh screen. 50 mL of 2 M NaOH and 10g of AS were mixed, and the mixture was stirred for 24 h at 30 °C. After adding 2.5g of ferrous sulphate (additive agent), mixture was stirred for 4 h. Following this, 10 mL of 10% gluteraldehyde (crosslinking agent) was added to the mixture and stirred for 30 min at room temperature. The filtered residue was washed with double-distilled water. The process was repeated until the filtrate's *p*H was close to neutral followed by oven drying for 12 h at 80 °C and named as MAS (modified almond shell). The FT-IR spectra as well as surface morphology of MAS was acquired both before and after adsorption. A digital *p*H meter was used for all *p*H measurements. A 100 ppm stock solution of the BG dye was prepared using deionised water. The Shimadzu 2600i spectrophotometer was used to detect the amounts of residual BG dye at 625 nm. Using BG solution at different concentrations (10, 20, 30, 40, 50, and 60 mg/L), a calibration curve was calculated. The effectiveness of MAS in adsorbing BG dye was investigated using batch studies. To optimize the *p*H, BG solutions (20 ppm, 20 mL) with varying *p*H values from 2 to 10 were prepared. BG solutions with several concentrations (20, 30, 40, 50, and 60 ppm) were prepared in order to optimize the initial concentration. Different adsorbent doses (0.2, 0.4, 0.6, 0.8, 1.0, 1.2, and 1.4 g) were added to the BG solution to optimise the adsorbent dose. For the optimisation of contact time and temperature, adsorption studies were carried out at different temperatures (20°C, 25°C, 30°C, 35°C, 40°C, 45 °C, 50 °C) for different contact times (30, 60, 90, 120, 150, 180 and 210 min). By conducting batch studies, the reaction parameters pH, dye solution concentration, amount of adsorbent, contact time, and temperature were optimised. As recommended by Kayan and Kayan (2007), the removal efficiency (%) and adsorptive capacity (qt) were determined using equation (1) and (2), respectively.

$$\text{Removal efficiency (\%)} = \frac{\text{Initial concentration} - \text{Final concentration}}{\text{Initial concentration}} \times 100 \quad \text{Eq. (1)}$$

$$\text{Adsorptive capacity} = \frac{\text{Initial concentration} - \text{Final concentration}}{\text{Initial concentration}} \times \text{Volume} \quad \text{Eq. (2)}$$

The experimental data were fitted into the Freundlich and Langmuir adsorption isotherms to ascertain whether the adsorption is physical or chemical. Kinetic modelling was performed by fitting the experimental data into the pseudo-first-order and pseudo-second-order kinetics.

Results and Discussion

FTIR (Fourier-transform-infrared) and FESEM (Field Emission Scanning Electron Microscopy) with EDS (EDAX-make)

The FTIR spectra of AS and MAS before and after dye adsorption are shown in figure1. The prominent hydroxyl group in AS, MAS, and BG loaded MAS has been ascribed to O–H and N–H stretching vibrations and is located between 3400 and 3457 cm^{-1}. Furthermore, peaks located between 2925, 2928 and 2936 cm^{-1} show that methyl and methylene groups exhibit C–H stretching vibrations (Ovchinnikov *et al.,* 2016).

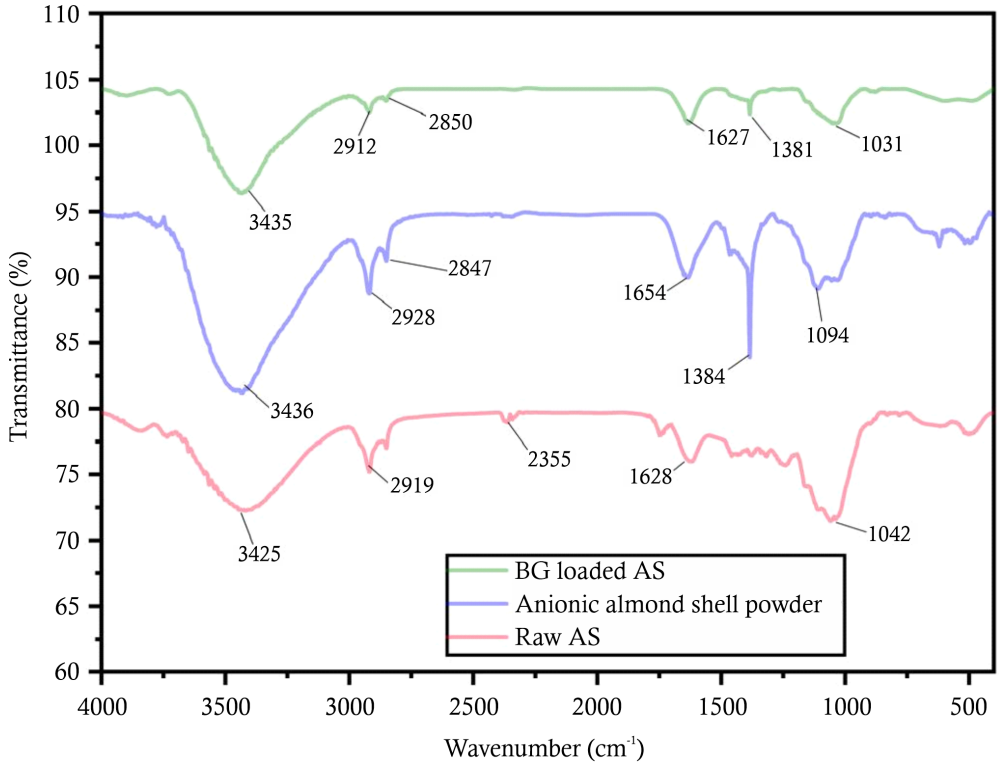

Fig. 1 FTIR spectra of (a) raw almond shell (WS); (b) chemically modified almond shell (MAS); (c) BG-loaded MAS

But compared with AS, the peak intensity was lower in MAS and BG-loaded MAS. Our results are consistent with the cited literature (Sudarsan *et al.*, 2025). FESEM and EDS scans are often employed to investigate the morphological properties of the adsorbent. Using a FESEM, the surface properties of WS, MAS, and BG dye-loaded MAS were studied (Figure 2a-b). The holes and irregularities on the MAS surface may have served as binding sites for BG dye during adsorption (Almeelbi, 2025). The adsorbent-absorbate interaction is confirmed by the surface alteration following modification (pretreatment) and dye adsorption process. After BG dye loading,

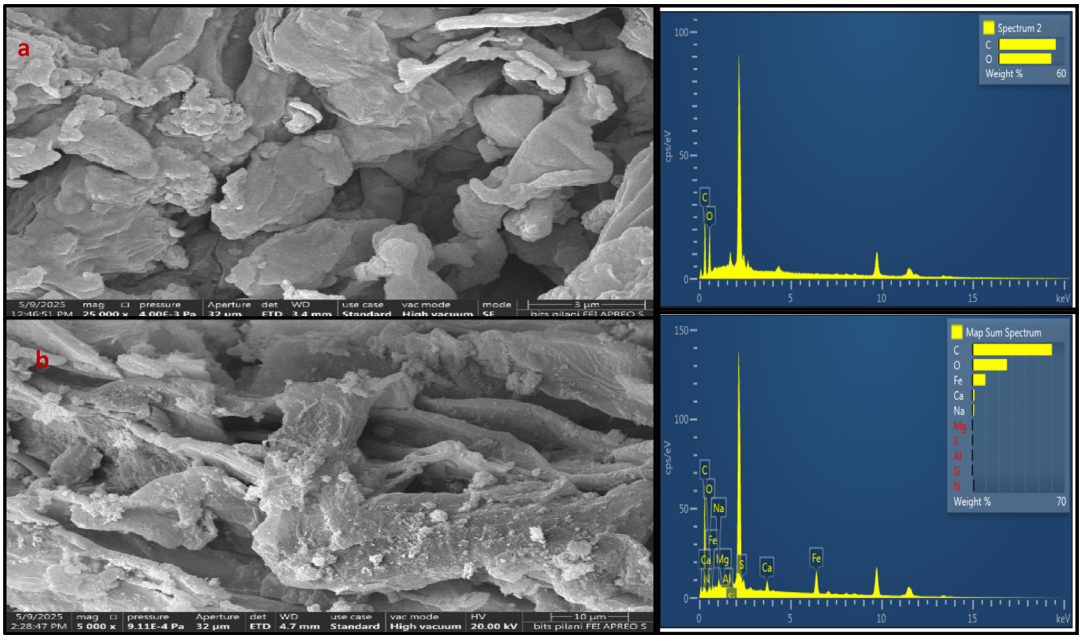

Fig. 2 FE-SEM micrograph of MAS (a) before (b) after BG dye adsorption

MAS's surface morphology significantly changes, with holes filled and covered as well as the shiny and appearance of a smooth surface becoming rough as in Fig. 2b (Muskan *et al.,* 2025). EDS provides evidence of the chemical change happened on adsorbent surface both before and after dye absorption.

Influence of *p*H

The impact of *p*H is a crucial parameter to analyse the surface interaction between the dye and the adsorbent. Figure 3a displays the BG adsorption efficiency of MAS at *p*H values ranging from 2 to 10. The optimal *p*H for BG dye removal was 8. After the BG dye solution reached its optimum *p*H, the removal efficiency stabilised because fewer adsorbent sites were available for adsorption. Nothing significantly changed after the *p*H was raised (Padidar and Mohammad, 2024). The functional groups become protonated and deprotonated by changes in solution pH, resulting in a charge on the biosorbent's surface (Kerrou *et al.*, 2023). Based on the adsorbent's point of zero charge (pH_{pzc}; Figure 3f), which was 7.0, the adsorbent surface carried a positive charge as the pH increased above pH_{pzc}, thereby decreasing the removal effectiveness of BG.

Effect of various initial dye concentrations

The concentration of dye plays a significant role in adsorption experiments, as it directly influences the adsorbent's adsorption capacity and efficiency. The removal efficacy of MAS was shown to decline steadily as BG dye concentration increased from 10 mg L^{-1} to 50 mg L^{-1}, at optimum pH and constant temperature and adsorbent dosage (Figure 3b). The maximum removal efficiency (%) of BG on MAS was observed at 30 mg L^{-1} of 84.4%. The removal efficiency increases up to a particular concentration; after that, the concentration increases and the dye adsorption decreases. At higher dye concentrations, the finite number of sites available for dye adsorption on the biosorbent surface (Nagpal *et al.*, 2025). The effect of BG dye concentration on activated carbon was investigated by Kumaravel et al. (2024), who found that when the dye concentration rises throughout the adsorption process, the amount of BG dye removed decreases.

Effect of adsorbent dose

The adsorbent dose plays a crucial role in the efficiency of adsorption processes, significantly influencing the removal capacity of contaminants from aqueous solution. At the initial dye concentration: (30 mg L^{-1}), *p*H: (8) at room temperature, the impact of adsorbent dosage on the removal efficiency of BG was investigated using varying amounts of adsorbents in the range of 0.2-1.0 g L^{-1}. The optimum adsorbent doses of BG was found to be 0.8 g L^{-1} with removal efficiencies of 81.2% (Figure 3c). The reason for the decline in removal effectiveness as the concentration of the adsorbent increases is the agglomeration of adsorbent particles, which reduces the active sites accessible for adsorption, as reported by Ojo *et al*. (2019). The saturation of adsorption at increasing adsorbent dosages is due to competition among dye molecules for available adsorption sites (Dovi *et al.*, 2021).

Influence of contact time

The contact time is a crucial parameter in adsorption experiments, as it determines the time required to reach equilibrium between the adsorbate and the adsorbent. The effect of contact time on dye removal by MAS was investigated to determine the equilibrium time. The impact of contact time on the removal efficiency of BG dye was investigated in the range of 20-120 min. The maximum adsorption for BG removal was observed at 120 min, with a maximum removal efficiency of 91.3% (Figure 3d). After the optimal time, equilibrium was attained, consistent with the literature reported by El-Emam *et al*. (2025) and Magdy *et al.* (2025). The rate of adsorption was initially fast because the dye ions were adsorbed onto the external surface of the modified samples (Kumari *et al.*, 2025).

Effect of temperature

Temperature plays a significant role in the adsorption process, influencing both the rate and capacity of adsorption. Five different temperatures in the range of 10 to 50° C were employed at the optimised parameters (Figure 3e).The maximum BG dye adsorption was found at 50°C, with a removal efficiency of 84.20%. The

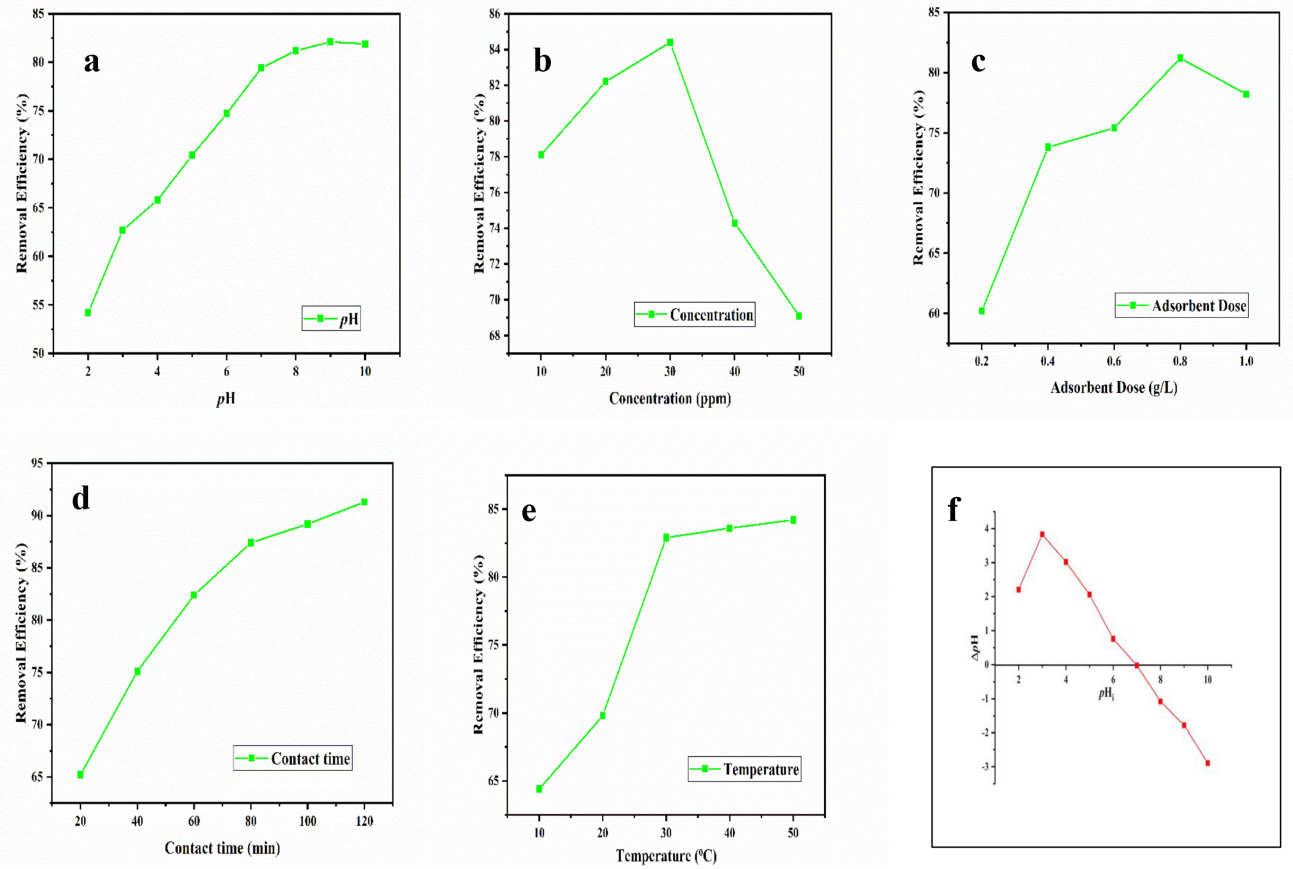

Fig. 3 Effect of (a) pH, (b) dye concentration, (c)adsorbent dose, (d) contact time, (e) temperature on BG dye adsorption and (f) point zero charge of MAS

adsorption efficiency increases with temperature due to increased mobility of brilliant green dye molecules (Aljeboree *et al.*, 2024). Temperature affects the adsorbent's adsorption capacity. It was found that an increase in temperature reduces the resistance of aqueous-phase viscous forces, thereby speeding up the diffusion of dye molecules through internal pores and the external boundary (Kali *et al.*, 2022). At higher temperatures, a decrease in removal efficiency was observed, as the adsorptive forces between dye molecules and biosorbents reduced adsorption capacity (Kulkarni *et al.*, 2023).

Adsorption isotherm models

The Freundlich and Langmuir isotherms are useful for explaining adsorption by various adsorbents (Langmuir, 1918; Freundlich, 1906). The nonlinear forms of the Langmuir and Freundlich equations are given in equations 3 & 4.

$$q_e = \frac{q_{max} b C_e}{1 + b C_e} \quad \text{Eq. (3)}$$

Where, q_{max} (mg g^{-1}) is the maximum monolayer adsorption capacity, b (L g^{-1}) is the Langmuir constant

$$q_e = k_f C_e^{1/n} \quad \text{Eq. (4)}$$

The adsorbent's adsorption capacity is denoted by k_f, its adsorption intensity is shown by the Freundlich constant 1/n, and its equilibrium concentration is represented by C_e, q_e is the total amount of dye molecule adsorbed/ total weight of adsorbents (mg g^{-1}), k_f (mg g^{-1}) is the Freundlich constant, and n is the heterogeneity factor that relates to the intensity of adsorption. As represented in Fig. 1, increased correlation coefficients (R^2) for the Langmuir model indicated that the adsorption data could be accurately explained by the Langmuir isotherm model. In the work of Agour *et al.* (2025), using

Table 1. Adsorption isotherm parameters for BG dye on MAS

Isotherm models	Parameters	Values
Langmuir	qmax (mg g^{-1})	121.73
	b (L mg^{-1})	0.15
	R^2	0.9963
Freundlich	1/n	0.5113
	Kf (mg g^{-1})	21.87
	R^2	0.9711

multifunctional copolymers for brilliant green dye removal, adsorption isotherm analysis showed a strong fit to the Langmuir model, with a maximum adsorption capacity of 16.28 mg g^{-1}. Our results are in agreement with that of the reported literature (Mchich *et al.*, 2025; Fayad *et al.*, 2025; Kumar *et al.*, 2025).

Kinetics Study

In this work, pseudo-1st- and pseudo-2nd-order models were employed to elucidate the kinetic behaviour of dye molecule adsorption onto MAS. The pseudo-first order is expressed in linear form in equation 5 (Samimi and Safari, 2022).

$$\log (q_e - q_t) = \log q_e - \left(\frac{k_1}{2.303}\right) t \qquad \text{Eq. (5)}$$

Here, q_e & q_t (mg g^{-1}) are the adsorption capacity at equilibrium time and at time t(min), respectively, k_1(min^{-1}) is the pseudo-first-order rate constant, and the value of k_1, q_e, and R^2 are calculated from a linear plot between log(q_e-q_t) vs t. Pseudo second order is in linear form is represented in equation 6 (Staron *et al.*, 2017).

$$\frac{t}{q_t} = \frac{1}{k_2 q^2 e} + \frac{t}{q_e} \qquad \text{Eq. (6)}$$

Here, k_2 (g mg^{-1} min^{-1}) is rate constant of pseudo second order. By plotting graph between t/q_t vs t we can calculate k_2, q_e, R^2 values. The q_e (exp) values from the adsorption experiment are compared to the q_e (cal) value calculated using the kinetic models. Figure presents the validation findings and the kinetics model parameters. The pseudo-second order regression coefficient is greater than the pseudo-first order regression coefficient, according to experimental data. Almond shell powder (ASP) as a natural low-cost adsorbent was evaluated in the batch adsorption kinetic study for the removal of brilliant green dye by varying pH, temperature, initial concentration of the dye, bioadsorbent dose, and contact time and the adsorption kinetics follow a pseudo-second-order model (Melhaoui *et al.*, 2025). Kinetic studies showed rapid sorption, following a second-order kinetic model, for the adsorption of organic dyes onto almond shells in the study by El-Khomri *et al.* (2022).

Thermodynamic studies

The thermodynamic parameters, including Gibbs free energy (ΔG^0), entropy change (ΔS^0) and enthalpy (ΔH^0) for the adsorption of BG dye, have been evaluated and verified using equations from 7 – 9 (Umeh *et al.*, 2024).

$$\Delta G^0 = -RT \ln k_d \qquad \text{Eq. (7)}$$

$$k_d = \frac{C_a}{C_e} \qquad \text{Eq. (8)}$$

$$\ln k_d = \frac{\Delta H^0}{RT} - \frac{\Delta S^0}{R} \qquad \text{Eq. (9)}$$

Here, k_d is the equation constant, R is the gas constant (8.314 J/mol/K), T is the temperature in K, and Ca is the amount of adsorbate on the adsorbent surface at equilibrium. ΔH^0 & ΔS^0 were determined from a linear plot between lnk_d vs

Table 2. Kinetics model parameters for BG dye on MAS

Kinetic models	Parameter	10 mg L^{-1}	20 mg L^{-1}	30 mg L^{-1}	40 mg L^{-1}	50 mg L^{-1}
PFO (linear)	$q_{e,cal}$(mg g^{-1})	66.96	10.79	17.85	10.15	19.68
	K_1 (min^{-1})	0.005	0.001	0.002	0.001	0.002
	R^2	0.5330	0.6674	0.8115	0.8966	0.9475
PSO (linear)	$q_{e,cal}$(mg g^{-1})	23.22	42.10	60.56	74.01	10.30
	K_2 (min^{-1})	0.003	0.004	0.003	0.004	0.001
	R^2	0.9907	0.9935	0.9989	0.9998	0.7619

Table 3 Thermodynamic parameters for for BG dye on MAS

Temperature (K)	1 T^{-1}	K_L	ln K_L	ΔG^0 ($KJmol^{-1}$)	R^2	ΔH^0 ($KJmol^{-1}$)	ΔS^0 ($JK^{-1}mol^{-1}$)
			AASP (FOR BG)				
293	0.0034	4.6428	1.5353	-3.7098	0.9965	18.9657	0.0773
303	0.0033	5.8518	1.7667	-4.4838			
313	0.0031	7.4469	2.0078	-5.2577			
323	0.0030	9.5772	2.2593	-6.0316			

1 T^{-1}. The increased randomness at the solid-solution interface is confirmed by positive ΔS^0 values, and the endothermic nature of the adsorption process is demonstrated by positive ΔH^0 values for the dye molecule via MAS (Muskan *et al*., 2025). The feasibility and spontaneity of the adsorption process are confirmed by negative ΔG^0 values for the dye molecule at increasing temperatures, indicating physical adsorption, as shown in Table 3 (Saini *et al*., 2025). Kali *et al*. (2022) reported that methylene blue adsorbed onto almond shells via an endothermic and spontaneous reaction. Jasrotia *et al.* (2024) stated that an endothermic, spontaneous reaction resulted in the adsorption of cationic dyes on nano ferrites modified with walnut shell.

Conclusions

The removal of BG from simulated water using MAS has been investigated under various experimental conditions in a batch. According to SEM images, the MAS surface is rich in pore structures, which facilitate the adsorption of BG molecules. The adsorption of dye molecules was influenced by the pH, dye concentration, adsorbent dosage, temperature and contact time. Based on adsorption studies, the dye molecule is removed at *p*H 7. The Langmuir isotherm was closely followed during the adsorption process by the adsorbent, and the adsorption kinetics followed pseudo-second order. The feasibility and spontaneity of the adsorption process are confirmed by the negative ΔG^0 values at increasing temperatures, indicating physical adsorption. The results of this study showed that Brilliant green may be successfully removed from an aqueous solution by using chemically modified almond shell.

References

Aggour Y A, Kenawy E R, Magdy M, and Elbayoumy E (2025) Multifunctional copolymers for brilliant green dye removal: adsorption kinetics, isotherm and process optimization. *Environmental Science Advances* **4(5):** 787–808.

Aljeboree A M, Alkaim A F, Hussein S A, Jawad M A, Hasan I, and Khuder S A (2024) Synthesis and swelling behavior of highly adsorbent hydrogel for the removal of brilliant green from an aqueous solution: thermodynamic, kinetic, and isotherm models. *Case Studies in Chemical and Environmental Engineering* **10:** 100831-100840.

Almeelbi T (2025) Magnetite biochar derived from date palm tree waste leaves for adsorption of Congo Red from aqueous solution. *Egyptian Journal of Chemistry* **68(9):** 205–212.

Dovi E, Aryee AA, Kani AN, Mpatani FM, Li J, Li Z, Qu L, and Han R (2021) Functionalization of almond shell by grafting amine groups to enhance the adsorption of Congo red from water in batch and fixed-bed column modes. *Journal of Environmental Chemical Engineering* **9(5):** 106301-106310.

El- Khomri M, El Messaoudi N, Dbik A, Goodarzvand Chegini Z, and Iqbal M 2022. Organic dyes adsorption on the almond shell (Prunus dulcis) as agricultural solid waste from aqueous solution in single and binary mixture systems. *Biointerface Research in Applied Chemistry* **12(2):** 2022–2040.

El-Emam D A, Elezaby A H, Zeyadah M A, and El-Sonbati M A (2025) Harnessing thermally treated drinking water sludge: a sustainable approach for the removal of crystal violet and congo red from wastewater. *Scientific Reports* **15(1):** 17426-17435.

Fayad E, Binjawhar D N, Elsaid F G, Taha A, and Mubarak M F (2025) Innovative CuZnCr-BTC framework for enhanced congo red dye removal in sustainable wastewater treatment. *Journal of Cluster Science* **36(4):** 125-132.

Freundlich HMF (1906) Over the adsorption in solution. *The Journal of Physical Chemistry* **57:** 385–470.

Jadhav J P, Kalyani D C, Telke A A, Phugare S S and Govindwar S P(2010) Evaluation of the efficacy of a

bacterial consortium for the removal of color, reduction of heavy metals, and toxicity from textile dye effluent. *Bioresour Technol* **101:** 165-174.

Jasrotia R, Singh R, Sharma D, Singh J, Mittal S, and Singh H (2024) A sustainable approach for enhancing cationic dyes adsorption in single and multiple systems using novel nano ferrites modified with walnut shell. *Chemistry Select* **9(18):** 4810-4820.

Kali A, Amar A, Loulidi I, Hadey C, Jabri M, Alrashdi A A, and Boukhlifi F (2022) Efficient adsorption removal of an anionic azo dye by lignocellulosic waste material and sludge recycling into combustible briquettes. *Colloids and Interfaces* **6(2):** 22-32.

Kali A, Dehmani Y, Loulidi I, Amar A, Jabri M, El-Kord A, and Boukhlifi F (2022) Study of the adsorption properties of an almond shell in the elimination of methylene blue in an aquatic. *Moroccan Journal of Chemistry* **10(3):** 509-522.

Kayan G O and Kayan A (2021) Composite of natural polymers and their adsorbent properties on the dyes and heavy metal ions. *Journal of Polymers and the Environment* 293477-293487.

Kerrou M, Raada S, Mrani D, and Elanssari A (2023) A comparative study of the adsorption of a cationic dye on three substrates. *Desalination and Water Treatment* **311:** 135–143.

Kulkarni K, Kurhade S, Chendake Y, Kulkarni A, and Satpute S (2023) Utilization of low cost biofertilizers for adsorptive removal of Congo Red Dye. *Bulletin of Environmental Contamination and Toxicology* **111(3):** 33-42.

Kumar N, Kumar V, and Garg V K (2025) Tailored synthesis of banana stem-derived activated carbon sponge for the efficient adsorption of industrial dye. *Next Materials* **8:** 100640-100649.

Kumaravel S Geetha M, Niyitanga T, Kumar D S, Al-Ansari M M, Mythili R, Suganthi S, Guganathan L, Murugan A, and Ragupathy S (2024). Preparation and characterization of activated carbon from corn cob by chemical activation and their adsorption of brilliant green dye from wastewater. *Process Safety and Environmental Protection* **188:** 1338-1345.

Kumari B, Chauhan S, Kumar K, Singh S and Chauhan G S (2025) Simultaneous removal of cationic and anionic dyes from a complex mixture using a novel composite hydrogel based on pine needles, chitosan, and gelatin. *International Journal of Biological Macromolecules* **307:** 141-147.

Langmuir I (1918) The adsorption of gases on plane surfacesof glass, mica and platinum. *Journal of American Chemical Society* **40:** 1361–1403.

Lima HHC, Maniezzo RS and Llop MEG (2019) Synthesis and characterization of pecan nutshell-based adsorbent with high specifc area and high methylene blue adsorption capacity. *Journal of Molecular Liquids* **276:** 570–576.

Magdy M, Aboelnga M M, Deyab Aemida A, Rizk R, Elseady N, Hashesh, M A, and Elbayoumy E (2025). Experimental and theoretical investigations of divinylbenzene-based polymer as an efficient adsorbent for brilliant green dye removal. *Rsc Advances* **15(25):** 19843–19858.

Manzoor K, Batool M, and Naz F (2024) A comprehensive review on application of plant-based bioadsorbents for Congo red removal. *Biomass Conversion and Biorefnery* **14:** 4511–4537.

Mchich Z, Kjidaa B, Bouzid T, Haddad M E, Mamouni R (2025) Engineering of highly bio-adsorbent Zinc Oxide/ Cellana Tramoserica seashells for efficient removal of anionic dye: BBD optimization, density functional theory study, and adsorption mechanism. *Separation and Purification Technology* **363:** 132015-132025.

Melhaoui R, Miyah Y, Kodad S, Houmy N, Addi M, Abid M, and Elamrani A (2021) On the suitability of almond shells for the manufacture of a natural low cost bioadsorbent to remove brilliant green: kinetics and equilibrium isotherms study. *The Scientific World Journal* **2021(1):** 665-678.

Miyah Y, Lahrichi A, Idrissi M, Khalil A and Zerrouq F(2018) Adsorption of methylene blue dye from aqueous solutions onto almond shells powder: equilibrium and kinetic studies. *Surfaces and Interfaces* **11(74):** 81-91.

Muskan, Kumari S, Shree B, Singh S, Manju, Rani I, and Dhanda A (2025) Application of modified walnut shell for adsorptive removal of anionic dye (Congo Red) from simulated water: Anionic dye removal using modified walnut shell as biosorbent. *Journal of Soil Salinity and Water Quality* **17(2):** 197-204.

Muskan, Kumari S, Singh S, BhagyaShree, Rani I, and Manju (2025) Modified almond shell for enhanced adsorption for methylene blue from aqueous solution: Preparation, characterisation, isotherm, kinetics and mechanism study. *Indian Journal of Chemical Technology* **32(3):** 313-323.

Nagpal M, Sharma N, and Mittal A (2025) Selective adsorptive removal and separation of harmful anionic dyes using mesoporous magnesium oxide-chitosan composite.*Hybrid Advances* **9:** 100393-100400.

Nandi B K, Goswami A, Purkait M K (2009) Adsorption characteristics of brilliant green dye on kaolin. *J. Hazard. Mater.* **161(1):** 387-395.

Nhat Ngo V N, Van Pham N, Tien M H, Vu Luong T H, Ngoc-Hanh C L, Thanh Q C, Dang G H (2026) Preparation of Fe3O4/ZIF-9 as an efficient heterogeneous nanocatalyst for brilliant green dye removal via advanced oxidation processes. *Journal of Physics and Chemistry of Solids* **209:** 113265-113275.

Ojo T A, Ojedokun A T and Bello O S (2019) Functionalization of powdered almond shell with orthophosphoric acid for Congo red dye removal. *Particulate Science and Technology* **37(1):** 74–85.

Ovchinnikov O V, Evtukhova A V, Kondratenko T S, Smirnov M S, Khokhlov V Y, and Erina O V (2016) Manifestation of intermolecular interactions in FTIR spectra of methylene blue molecules. *Vibrational Spectroscopy* **86:** 181-189.

Padidar A and Mohammadi A (2024) Development of a magnetite nanocomposite based on expanded graphite/ chitosan for efficient removal of brilliant green dye from aqueous solutions. *Separation Scienceand Technology Philadelphia* **59(6-9):** 954–966.

Roy K, Verma K M , Vikrant K, Goswami M, Sonwani R K, Rai B N, Vellingiri K, Kim K H, Giri B S, Singh RS (2018) Removal of patent blue (V) dye using Indian bael shell biochar: characterization, application, and kinetic studies. *Sustainability* **10:** 2669-2680.

Sahu A and Poler J C (2024) Removal and degradation of dyes from textile industry wastewater: Benchmarking recent advancements, toxicity assessment and cost analysis of treatment processes. *Journal of Environmental Chemical Engineering* **1(11):** 3754-3760.

Saini P, Chakinala N, Praveen K Surolia, Gupta A and Chakinala (2025) Ultrasound-assisted enhanced adsorption of textile dyes with metal organic frameworks. *Separation and Purification Technology* **354:** 128730-128740.

Samimi M and Safari M (2022) TMU-24 (Zn-based MOF) as an advance and recyclable adsorbent for the efficient removal of eosin B: characterization, equilibrium, and thermodynamic studies. *Environmental Progress & Sustainable Energy*, 1–9.

Staron P, Chwastowski J, Banach M (2017) Sorption and desorption studies on silver ions from aqueous solution by coconut fiber. *The Journal of Cleaner Production* **149:** 290–301.

Sudarsan S, Murugesan G, Varadavenkatesan T, Vinayagam R, and Selvaraj R (2025). Efficient adsorptive removal of Congo Red dye using activated carbon derived from *Spathodea campanulata* flowers. *Scientific Reports* **15(1):** 1831-1840.

Umeh CT, Nduka JK, Mogale R, Akpomie KG, Okoye NH (2024) Acid-activated corn silk as a promising phytosorbent for uptake of Malachite green and Cd (II)ion from simulated wastewater: equilibrium, kinetic andthermodynamic studies.*International Journal of Phytoremediation* **26(10):** 1593-1610.

Xu L, Zheng X, Cui H, Zhu Z, Liang J and Zhou J (2017) Equilibrium, kinetic, and thermodynamic studies on the adsorption of cadmium from aqueous solution by modified biomass ash. *Bioinorg Chem Appl,* 1–9.

Zhao H, Yu Q, Li M, and Sun S(2020) Preparation and water vapor adsorption of "green" almond-shell activated carbon by CO2 physical activation. *Adsorption Science Technology* **38:** 60–76.

Received: February 07, 2026; Accepted: March 14, 2026